

Chemistry of dense clumps near moving Herbig-Haro objects

H.Christie^{1*}, S.Viti¹, D.A.Williams¹, J. M. Girart², O. Morata³

¹*Department of Physics and Astronomy, UCL, Gower street. London WC1E 6BT,*

²*Institut de Ciències de l'Espai (CSIC-IEEC), Campus UAB, Facultat de Ciències, Torre C5 - parell 2, 08193 Bellaterra, Catalunya, Spain,*

³*Institute of Astronomy & Astrophysics, Academia Sinica, P.O. Box 23-141, Taipei 10617, Taiwan*

18 February 2022

ABSTRACT

Localised regions of enhanced emission from HCO^+ , NH_3 and other species near Herbig-Haro objects (HHOs) have been interpreted as arising in a photochemistry stimulated by the HHO radiation on high density quiescent clumps in molecular clouds. Static models of this process have been successful in accounting for the variety of molecular species arising ahead of the jet; however recent observations show that the enhanced molecular emission is widespread along the jet as well as ahead. Hence, a realistic model must take into account the movement of the radiation field past the clump. It was previously unclear as to whether the short interaction time between the clump and the HHO in a moving source model would allow molecules such as HCO^+ to reach high enough levels, and to survive for long enough to be observed. In this work we model a moving radiation source that approaches and passes a clump. The chemical picture is qualitatively unchanged by the addition of the moving source, strengthening the idea that enhancements are due to evaporation of molecules from dust grains. In addition, in the case of several molecules, the enhanced emission regions are longer-lived. Some photochemically-induced species, including methanol, are expected to maintain high abundances for $\sim 10^4$ years.

Key words: Herbig-Haro object

1 INTRODUCTION

Herbig-Haro objects are knots of optical emission, produced when the jet from a young star collides with the ambient interstellar material to produce a shock front (Falle & Raga 1993). These Herbig-Haro objects (HHOs) are strong line emitters at optical and other wavelengths and are often seen along a protostellar outflow as a series of bow shocks moving away from the star. A number of observational surveys have detected localised regions of enhanced emission in several molecules, among them NH_3 and HCO^+ , just ahead of Herbig-Haro objects (Girart et al. 1994; Girart, Estalella & Ho 1998, Torrelles et al. 1992). The regions appear chemically similar to each other and are quiescent and cool. Therefore they are probably dynamically unaffected by the jet. Girart et al. (1994) suggested that emission may be from molecules in icy mantles on dust being released by UV radiation from the Herbig-Haro object. Taylor & Williams (1996) supported this theory with a simple chemical model which reproduced the abundances inferred from observations of these quiescent regions. A more complex chemical model

was then investigated by Viti & Williams (1999) and used to predict other molecular species expected to show enhanced emission under the same conditions. Many of these, including CH_3OH , H_2CO and SO_2 , were later observed both in clumps ahead of HH2 (Girart et al. 2002) and near to five other Herbig-Haro objects (Viti et al. 2006).

The model used by Viti & Williams (1999), Girart et al. (2002) and Viti et al. (2003) described the particular photochemistry that is produced when radiation from these HHOs impinges on clumps of gas, located ahead of the bow shock, in which ices have returned to the gas phase. In particular, the HHO (and hence the source of UV radiation) was assumed to be static. However, recent observations of the object HH43 (Morata et al. in preparation) reveal the presence of several molecular species *along* the jet, where at least three HH objects are present (see Figure 1). From the H^{13}CO^+ emission it is clear that the emission is in clumps or small filaments along the outflow and that they are quiescent (as they show narrow line widths). HCO^+ and CS emission also show such distinct clumps, and, consistent with previous observations of clumps ahead of HH objects, there seems to be a stronger contrast in intensity between clumps and elsewhere nearby in HCO^+ than in CS (consistent also with

* E-mail: hc@star.ucl.ac.uk

the fact that CS should trace larger scale gas). These observations seem to indicate that quiescent clumps, chemically (but not dynamically) affected by the HH object, are present *along* the jet and not only ahead as previous surveys indicated. While previous modelling was successful at providing an explanation for the chemical enhancement ahead of the HHO, what is now required is a model that can explain different degrees of chemical quiescent enhancements along the jet. The model needs therefore to be dynamical in order to take into account the movement of the shock front, typically travelling at a few hundred kms^{-1} through a molecular cloud. Raga & Williams (2000) investigated, using a simple chemistry, the effect of a moving field on the expected morphology of the emission but the full consequences on the chemistry of allowing the radiation source to move have not been explored.

In this scenario, the HHO (the source of the radiation driving the photochemistry) approaches a clump and then passes it, so that the radiation intensity rises to a peak value and then decays. In this work we explore how the chemistry induced in the clump differs from that in the static case previously discussed, and consider the sensitivity of the chemistry to assumed geometry and physical conditions. Figure 1 suggests that in HH43 a clump may be affected by the passage of more than one HHO. However, in this work we examine the photochemistry induced by a single HHO passage.

Figure 1 shows the HH 38-43-64 system in emission lines of several molecular species. This system of HHOs is initiated by a source, HH 43 MMS1, indicated by a cross in the figure. The source appears to have initiated several HHO events, but in our treatment we consider only a single event. The figure shows clearly that emitting molecules are distributed along the line of the jet, and are not confined to discrete objects in front of the jet head.

2 THE MODEL

The basic model used is that of Viti & Williams (1999) and Viti et al. (2002) which runs in two phases, the first simulating the collapse of molecular cloud gas from a fairly diffuse state to a clump of uniform high density, and the second the illumination of the clump by a static radiation source.

In the model, the clump is treated as a one-dimensional slab of fixed temperature, increasing in visual extinction throughout up to a maximum value representing the clump centre. Abundances are calculated for 10 depth points through the slab. We assume the clump to be spherically symmetric and the radiation field to be isotropic at the clump surface so that the 1D slab is able to represent the whole clump. Using classic rate equations and the abundances in the previous time step, abundances of species are calculated at each depth point and for each time step (the gap between time steps is varied according to how quickly abundances are likely to be changing). This way the chemistry of the whole clump is tracked for the duration of the model run. Self-shielding of molecular hydrogen and CO is taken into account so that photodissociation of these species depends on the abundances in outer depth points.

The model follows the chemical evolution of 170 species including 1858 separate reactions for the 10 depth points of

increasing visual extinction (A_v). Reaction rates are taken from the UMIST database (Woodall et al. 2007).

During phase I the clump undergoes a modified free-fall collapse during which molecules are allowed to freeze-out or deplete onto dust grains, where they undergo hydrogenation as far as possible. Ions are neutralized on hitting the grain surface and reaction rates on the surfaces take into account the small negative charge on the dust grains resulting in a slightly higher rate for the positive ions. The radiation field in phase I is fixed at 1 Habing to represent the ambient interstellar field.

Depletion of species from the gas phase as they are frozen out onto grains is controlled within the model by effectively altering the grain surface area available for gas species to freeze-out. The freeze-out fraction of CO at the end of phase I was set to around 20% for models with a final clump density of 10^4 cm^{-3} (regardless of the initial clump density), around 50% for final densities of 10^5 cm^{-3} and 70% for final densities of 10^6 cm^{-3} . These values are consistent with observational depletion studies of isolated dark clouds, where denser objects show a higher degree of freeze-out of CO (eg. Redman et al. 2002). All models assumed that 5% of the CO freezing out onto the grains was converted into methanol.

The initial number density of hydrogen nuclei in the clump (before collapse) is assumed to be 10^3 cm^{-3} . It is also assumed that, initially, only carbon is ionised and half of the hydrogen is in its molecular form. Nitrogen, oxygen, magnesium, sulphur and helium are all neutral and atomic. As assumed by Viti & Williams (1999), the first phase continues until a specified number density is reached. This number density is observationally determined to be in the range 10^4 to 10^5 cm^{-3} (e.g. Girart et al. 2005; Whyatt et al. 2010). We have also explored the effect of allowing somewhat higher densities in several models (see Table 1). For simplicity, the clump is assumed to be of uniform density at all times.

The second phase commences immediately after the specified density is attained, when it is assumed that the radiation from the HHO is switched on. There is no collapse in this phase, the clump remains at a constant density (equal to that at the end of phase I) and a constant temperature throughout. The HH radiation field is again isotropic but stronger than the ambient field irradiating the clump in phase I. The chemistry in the second phase is then computed for a model time of about a million years.

The radiation field of the HHO is represented in the model in terms of multiples, G_0 , of the mean interstellar radiation field intensity. This is clearly an approximation, since the spectra of the two fields are not the same. Unfortunately, all astrochemical codes use the interstellar field as the basis of their treatments of photo-processes, and to do otherwise would be a major project beyond the scope of this work. While the approximation we have used could give misleading results, the prediction of a rich characteristic photochemistry in HHO-illuminated clumps (Viti & Williams 1999) has been confirmed by observations of a number of sources (Girart et al. 2002, 2005, Viti et al. 2006) and by a very detailed study of HH2 (Girart et al. 2005).

In the adapted model, the moving source of this radiation field (representing the HHO) passes the clump on a straight path with a minimum distance to the edge of the clump, here chosen to be 0.05 pc. This distance is similar

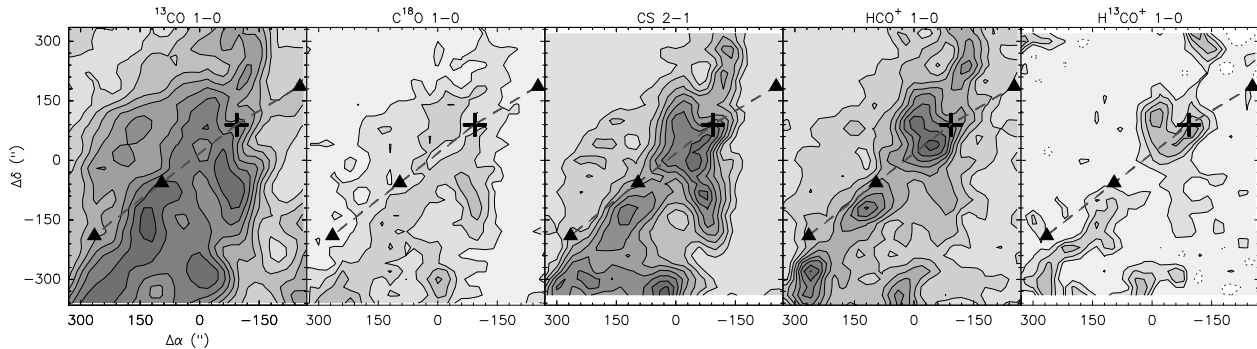


Figure 1. Integrated emission of some molecular line transitions in the $6.2\text{--}7.2\text{ km s}^{-1}$ v_{LSR} range, where emission (especially in HCO^+) follows HH 38-43-64 outflow. The molecular line transition is shown on the top of each panel. For the C^{18}O and H^{13}CO^+ panels, the contour levels are from 25% to 95% of the peak intensity in steps of 20%. For the other panels the contour levels are from 25% to 95% of the peak intensity in steps of 10%. The triangles show, from left to right, the Herbig-Haro objects HH 38, HH 43 and HH 64. The cross shows the position of HH 43 MMS 1, where the powering source of the HH system is located (Stanke, McCaughrean & Zinnecker 2000). Note that the two well defined clumps in HCO^+ ahead and south of HH 43 and HH38 have narrow lines ($\Delta v \simeq 0.7\text{ km s}^{-1}$), which suggests that they are dynamically quiescent.

to values found by Whyatt et al. (2010) in an observational study of regions around 22 HHOs. For a source moving at 300 km s^{-1} , there will be enough time for it to reach closest approach (at around 1000 years) and move some distance away before phase II is terminated. There is a range of values observed for HHO velocities from ~ 100 to $\sim 1000\text{ km s}^{-1}$. Faster HHOs have a shorter interaction time. We have used 300 km s^{-1} for most of the models considered, but have also explored the effects of a higher velocity in models 16-18 (see Table 1). The flux reaching the edge of the clump is time-dependent, changing with the distance from source to clump and reaching a specified peak value. Absorbing material along the line of sight to the clump is represented by an A_v of 1 magnitude at the clump edge. This low extinction material will, in any case, have little effect on the model outputs. Models with a static radiation source (kept at 0.05 pc from the clump throughout phase II) were run for comparison.

The main parameters affecting the model chemistry are the density of the molecular cloud from which the clump forms in phase I and the density of the clump at the end of phase I; the final clump radius which, along with the density, will determine the visual extinction, A_v , of the clump; the radiation peak strength of the field from the Herbig-Haro object at the clump boundary; and the source velocity. The values of these parameters adopted for each model are shown in Table 1. We also ran a few models to represent the interclump medium, i1, i2 and i3, with an initial density in phase I of 10^2 cm^{-3} and a final density of 10^3 cm^{-3} . No freeze-out occurs in either phase for the interclump models and phase I is extended for a time after the final density is reached. The relative radiation strengths, G_0 , listed in Table 1 are up to a few tens; these are the strengths found in previous modelling work (Viti & Williams 1999) to be necessary to create the rich variety of photochemistry subsequently observed by Girart et al. (2002) and Viti et al. (2006). Elemental abundances, adapted from Sofia & Meyer (2001), are listed in Table 2.

Column densities are calculated by summing fractional

Table 1. Model Input Parameters

Model Number	Initial Cloud Density (cm^{-3})	Final Clump Density (cm^{-3})	Clump Radius (pc)	Radiation Field Strength (G_0)	Source velocity (km s^{-1})
i1	10^2	10^3	3	5	300
i2	10^2	10^3	3	20	300
i3	10^2	10^3	3	30	300
1	10^3	10^4	0.3	5	300
2	10^3	10^4	0.3	20	300
3	10^3	10^4	0.3	30	300
4	10^3	10^5	0.03	5	300
5	10^3	10^5	0.03	20	300
6	10^3	10^5	0.03	30	300
7	10^4	10^5	0.03	5	300
8	10^4	10^5	0.03	20	300
9	10^4	10^5	0.03	30	300
10	10^4	10^6	0.003	5	300
11	10^4	10^6	0.003	20	300
12	10^4	10^6	0.003	30	300
13	10^3	10^4	0.3	50	300
14	10^3	10^5	0.03	50	300
15	10^4	10^6	0.03	50	300
16	10^3	10^5	0.03	5	1000
17	10^3	10^5	0.03	20	1000
18	10^3	10^5	0.03	30	1000

abundances at all 10 depth points for each species, taking into account the value of A_v at each point.

3 RESULTS

Our results are summarized in Figures 2 and 3. While we find that the fractional abundances of a given species in the gas surrounding an Herbig-Haro object are clearly different between the ‘moving’ and ‘static’ cases, it is clear

Table 2. Initial elemental abundances (from Sofia & Meyer 2001)

Element	Initial abundance (X(N)/X(H))
Helium	0.075
Carbon	1.79×10^{-4}
Oxygen	4.45×10^{-4}
Nitrogen	8.52×10^{-5}
Sulphur	1.43×10^{-6}
Magnesium	5.12×10^{-6}

Table 3. Comparing the effects of moving and static sources for model 5 with the clump at an A_v of 5 magnitudes. E denotes early times, L late times (after around 300 years). Up arrows indicate molecules that increase in abundance with a moving source rather than static, right arrows those that do not change and down arrows those that decrease in abundance.

Very Strongly Affected			Strongly Affected			Weakly Affected			Not Affected		
Mol	E	L	Mol	E	L	Mol	E	L	Mol	E	L
CH ₃ OH	→	↑	OCS	→	↑	CN	→	↓	H ₂ CO	↓	↓
NH ₃	→	↑	HC ₃ N	↑	↑	HCN	↑	→	HCO	↓	↑
SO ₂	↓	↑	C ⁺	↓	↓	C ₃ H ₅ ⁺	↑	→	CS	→	↓
SO	↓	↑	OCN	↓	↑	H ₂ CN	↑	↓	HCO ⁺	↑	↓
H ₂ S	→	↑	NS	→	↑	HNC	↑	↓			
			CH ₃ CN	→	↑	HCS ⁺	↑	↓			
			C ₃ H ₄	↑	→	H ₂ CS	↓	↑			
			CO	↓	→	NO ⁺	→	↑			
			C ₂ H	↑	↑	C	↓	↓			

that the theory proposed by Viti & Williams is still valid, even if the radiation source is moving with respect to the clumps. In fact, some species seem to survive longer if a moving source is included. Figure 2 plots column densities of four selected species throughout phase II. Both the moving and static source models are shown as well as column densities for the interclump medium, also under the influence of moving and static fields. The four species included in Figure 2 were selected because their abundances were particularly altered by a moving source or because they are particularly important observationally. Discrepancies were largest for lower A_v (smaller or more diffuse clumps) but similar for radiation field strengths in the range 5-50 G_0 , so the fact that the radiation source is moving is important, regardless of field strength. Table 3 compares the effects of moving and static sources for several observationally important species. Species whose abundances differ at least three orders of magnitude at any point in phase II between the moving and static cases are considered very strongly affected by the presence of the moving field. Where abundances differ at least two orders of magnitude but less than three, species are considered strongly affected. If abundances differ at least one order of magnitude and less than two, species are considered weakly affected and where abundances differ less than one order of magnitude between the two cases species are considered unaffected. Table 3 refers to model 5 with A_v of 5 magnitudes. Arrows indicate the way in which the moving source affects the abundance of each species both at early times and later, during the passage of the HHO.

Table 4. Timescales of abundance enhancements - Model 5. Timescale defined as the time taken for column density to drop below 10^{12} cm^{-2} or to stop falling.

Molecule	Timescale (Moving)	Timescale (Non-moving)
CH ₃ OH	10^5 yrs	10^3 yrs
NH ₃	10^5 yrs	10^4 yrs
SO	10^6 yrs	5×10^5 yrs
HCO ⁺	5×10^3 yrs	5×10^3 yrs
CN	10^5 yrs	10^5 yrs
HCN	10^6 yrs	5×10^5 yrs
CS	5×10^6 yrs	5×10^5 yrs
OCS	5×10^6 yrs	10^3 yrs
CO	10^6 yrs	10^5 yrs
NS	10^6 yrs	10^6 yrs
H ₂ CO	10^6 yrs	5×10^5 yrs
H ₂ S	5×10^4 yrs	5×10^3 yrs
H ₂ CS	5×10^6 yrs	5×10^5 yrs

In general, including a moving source implies that the radiation field decays quickly enough that the chemistry is being driven more slowly. This way the specially created species arising in the photochemistry survive for longer. For most of the strongly affected species, with a moving radiation source, column densities may remain high at least up to 30,000 years (and possibly much longer) after the passage of the source. Table 4 illustrates this point: here we list the length of time selected species survive for both the static and moving source cases.

Most species chosen for the study are first enhanced and later destroyed by the radiation field and hence show similar behaviour under the influence of a moving source. Their abundances are marginally lower than for the static field for up to a few hundred years (in which time the HHO moves only a very small distance) but later, as species begin to be destroyed by the radiation, the abundances in the moving case remain higher for longer. In some cases the chemistry appears to be such that abundances may not return to their initial values for long periods. CH₃OH, H₂S and NH₃ have higher abundances in the moving case than in the static case for the evolutionary time shown in Figure 2. C and C⁺ are enhanced by the radiation field and abundances are lower at all times in the moving case. HCO⁺ and HCS⁺ have higher abundances in the moving case at very early times but drop more later and are lower than for the static field at later times.

Models 13-15 were run with a 50 G_0 field. The changes in abundances are similar to models with a weaker field although more extreme, with elements such as CH₃OH and NH₃ decreasing in abundance at late times. This is illustrated in Figure 3 which shows the effect (on HCO⁺) of altering A_v , field strength, shock velocity and final clump density on the model output in phase II.

It appears counter intuitive that the density affects the abundance of HCO⁺ in the opposite sense to the A_v . However, because the A_v for the different density models is fixed (at around 6 magnitudes for the innermost depth point) the radiation field penetrates to the same extent in all models. The difference in abundance thus arises from differences in

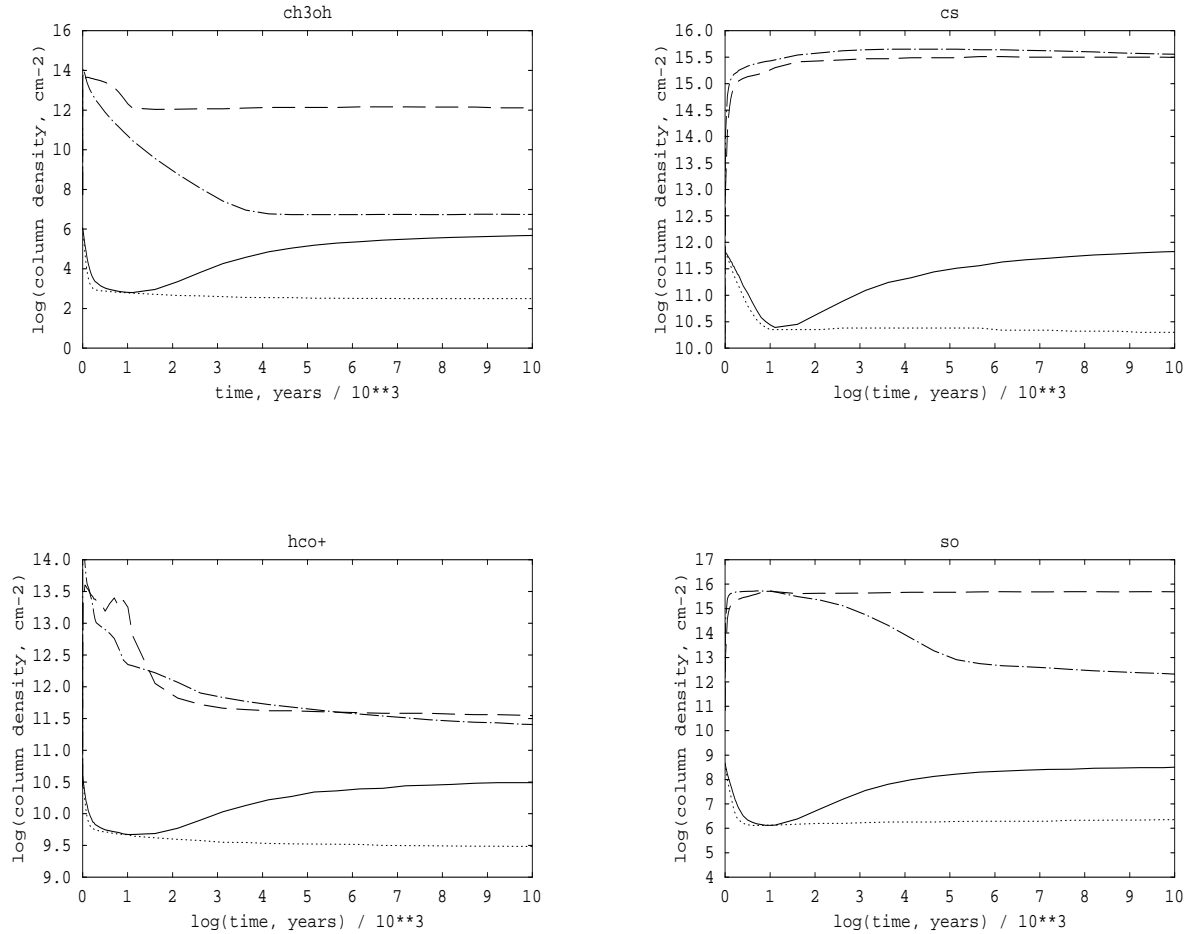


Figure 2. Column density (cm^{-2}) versus time (years). The solid black line represents the interclump medium, $A_v \sim 2$ mags, irradiated by a moving field of 30 G_0 (model i3), dashes - a clump at 10^5 cm^{-3} , $A_v \sim 5$ mags, irradiated by a moving field of 30 G_0 (model 6), dots - the interclump medium, $A_v \sim 2$ mags, irradiated by a static field of 30 G_0 (model i3 with a static field) and dots and dashes - a clump at 10^5 cm^{-3} , $A_v \sim 5$ mags, irradiated by a static field of 30 G_0 (model 6 with a static field). In the moving case the radiation field source is at its closest point at around 1000 years.

reaction rates due to the density of material for the main reactions forming and destroying HCO^+ . These are, respectively, the recombination of CH and O and the recombination of HCO^+ with electrons.

The influence of the radiation source speed on the model output was investigated in models 16-18 (again see Figure 3). It appears that a faster moving source allows several important molecular species to sustain, up to 30,000 years at least, higher column densities than in the case of a 300 km s^{-1} shock. Generally, the effects are seen later than about 300 years.

4 CONCLUSIONS

Clumps containing enhanced molecular abundances are routinely observed near Herbig-Haro objects (HHOs) in low-mass star-forming regions. The characteristic chemistry displayed by these clumps is consistent with a model in which the gas of evaporated ices is subjected to a photochemistry driven by the nearby HHO. Previous models have been successful in reproducing the variety in the observed chemical species; however, it was not obvious that they could explain the observed clumps along a jet which would be subject to a varying radiation field during the passage of the HHO. Moreover, the chemical effects in previous models were transient on a short timescale so that clumps were required to be extremely young and short-lived, causing some concern. In this work, we investigate the effect of adapting the earlier

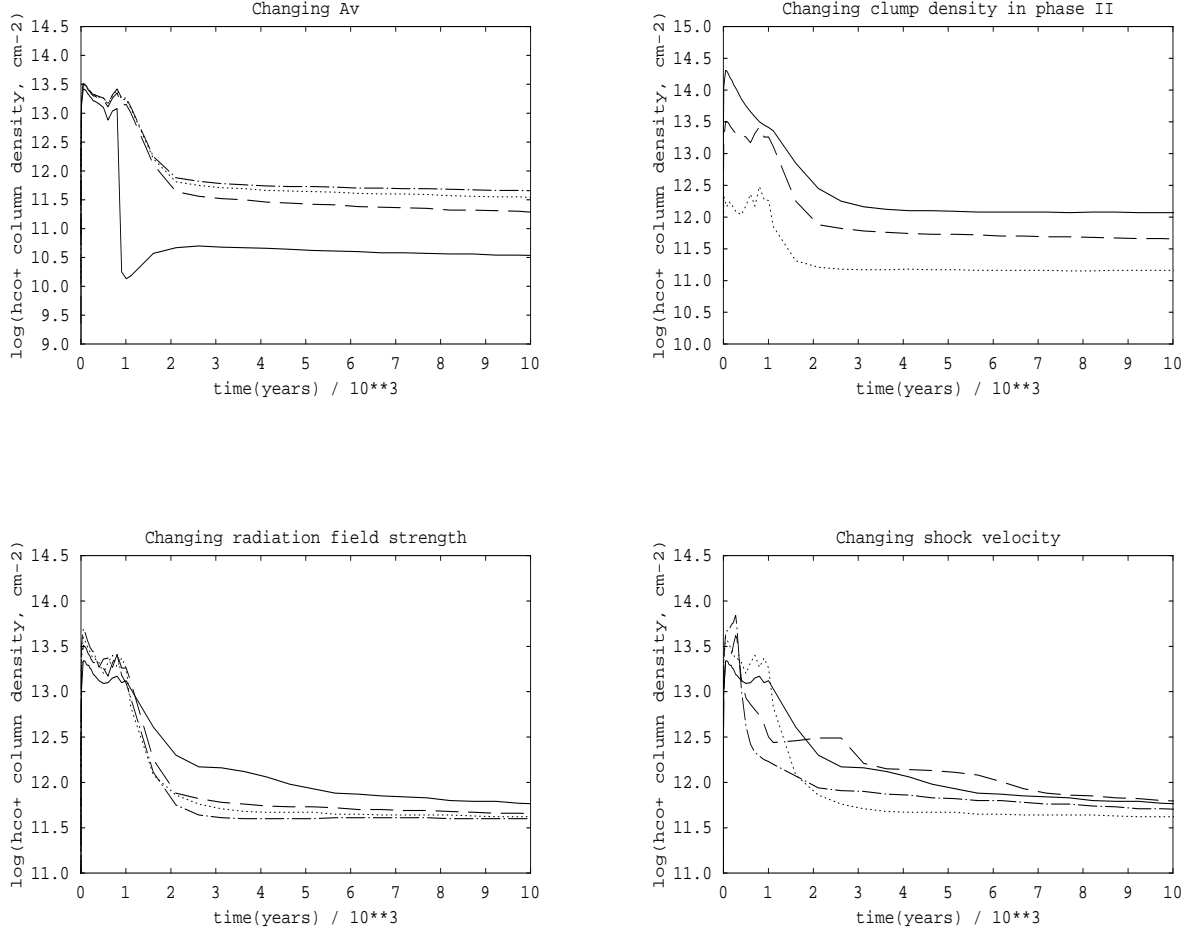


Figure 3. For HCO^+ . Top left plot - varying A_v : solid line represents a clump at 10^5 cm^{-3} with a moving source of 20 G_0 (model 5) at 1 mag, dashes - 3 mags, dots - 4 mags, dots and dashes - 6 mags. Top right hand plot - varying clump density: solid line represents model 2 (10^4 cm^{-3} with a moving source of 20 G_0), dashed line - model 5 (10^5 cm^{-3}), dotted line - model 11 (10^6 cm^{-3}). Lower left hand plot - varying radiation field strength: solid line represents model 4 (5 G_0), dashed line - model 5 (20 G_0), dotted line - model 6 (30 G_0) and single dots and dashes - model 14 (50 G_0). Bottom right hand plot - varying shock velocity: solid line represents model 4 (5 G_0 at 300 kms^{-1}), dashed line - model 16 (5 G_0 at 1000 kms^{-1}), the dotted line - model 6 (20 G_0 at 1000 kms^{-1}) and dots and dashes - model 18 (30 G_0 at 1000 kms^{-1}). Apart from the top left hand plot $A_v \sim 6$

models to include a moving, rather than static, radiation source. The main conclusions of the work are as follows:

- Results from the moving source model confirm that it is still possible to reproduce the particular chemistry observed in clumps near to HHOs while allowing the radiation source to move rather than remain static relative to the clump. This supports the idea that emission is due to the evaporation of species frozen out onto dust grains in dense regions of a molecular cloud.

- The new model enables several important molecules to maintain detectable abundances for longer periods.

- Species can be grouped into roughly three categories displaying similar behaviour under the influence of the moving source. Some (such as CH_3OH , NH_3 and H_2S) have much higher abundances at all times with a moving source than

with a static source. Most species investigated (including SO_2 , SO , NO^+ , HCO^+ , HCN , CN , CS and OCS) are first formed and then destroyed by reactions initiated by the radiation field and hence are less abundant with the moving field up to about 1000 years (for a source moving at 300 kms^{-1}) and then more abundant (this is most apparent for lower A_v clumps, hence is not obvious in figure 2 which plots those of higher A_v). C^+ and C abundances are enhanced by the field and are lower with the moving field at all times.

- Species with most noticeably increased abundances in the ‘moving’ case (as opposed to the ‘static’ case) are CH_3OH , NH_3 , SO_2 , SO and H_2S .

- The discrepancy between the moving and static cases is greater for a faster moving, stronger source and clumps of smaller size or lower density.

The results of this investigation support the idea that the observed chemistry ahead of Herbig-Haro objects is a result of species on the grains returning to the gas phase. The moving source allows the chemistry to persist for longer, helping to explain the large number of these clumps observed.

ACKNOWLEDGEMENTS

H.C. thanks Dermot Madden for help with coding and the STFC for funding.

REFERENCES

- Falle S.A.E., Raga A.C., 1993, MNRAS, 261, 573
 Garrod R.T., Williams D.A., Rawlings J.M.C., 2006, ApJ, 638, 827
 Girart J.M., Estalella R., Ho P.T.P., 1998, ApJ, 495, 59
 Girart J.M., Rodriguez L.F., Anglada G., et al., 1994, ApJ, 435, 145
 Girart J.M., Viti S., Williams D.A., Estalella R., Ho P.T.P., 2002, A&A, 388, 1004
 Girart J.M., Viti S., Estalella R., Williams D.A., 2005, A&A, 435, 113
 Herbig G.H., Jones B.F., 1983, ApJ, 88, 1040
 Morata O., Girart J.M., Estalella R., 2003, A&A, 397, 181
 Gilman R.C., 1972, ApJ, 178, 423
 Raga A.C., Williams D.A., 2000, A&A, 358, 701
 Redman M.P., Rawlings J.M.C., Nutter D.J., Ward-Thompson D., Williams D.A., 2002, MNRAS, 337, 17
 Ruffle D.P., Hartquist T.W., Caselli P., Williams D.A., 1999, MNRAS, 306, 691
 Sofia U.J., Meyer D.M., 2001, ApJ, 554, 221
 Stanke T., McCaughrean M.J., Zinnecker H., 2000, A&A, 355, 639
 Taylor S.D., Williams D.A., 1996, MNRAS, 282, 1343
 Torrelles J.M., Rodriguez L.F., Canto J., ApJ, 396, 95
 Viti S., Girart J.M., Garrod R.T., Williams D.A., Estalella R., 2003, A&A, 399, 187
 Viti S., Girart J.M., Hatchell J., 2006, A&A, 449, 1089
 Viti S., Williams D.A., 1999, MNRAS, 310, 517
 Whyatt W., Girart J.M., Viti S., Estalella R., Williams D.A., 2010, A&A, 510, 74
 Woodall J., Agundez M., Markwick-Kemper A.J., Millar T.J., 2007, A&A, 466, 1197